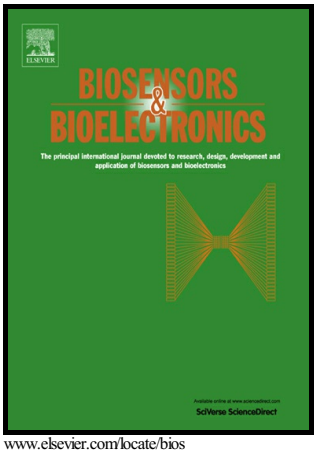

www.elsevier.com/locate/bios

Using the Rubik's Cube to directly produce paper analytical devices for quantitative point-of-care aptamer-based assays

Haiyan Fu, Juanhua Yang, Lin Guo, Jinfang Nie, Qiaobo Yin, Lang Zhang, Yun Zhang

PII: S0956-5663(17)30323-8
DOI: http://dx.doi.org/10.1016/j.bios.2017.05.012
Reference: BIOS9724

To appear in: *Biosensors and Bioelectronic*

Received date: 17 February 2017
Revised date: 15 April 2017
Accepted date: 5 May 2017

Cite this article as: Haiyan Fu, Juanhua Yang, Lin Guo, Jinfang Nie, Qiaobo Yin Lang Zhang and Yun Zhang, Using the Rubik's Cube to directly produce pape analytical devices for quantitative point-of-care aptamer-based assays, *Biosensor and Bioelectronic,* http://dx.doi.org/10.1016/j.bios.2017.05.012

Using the Rubik's Cube to directly produce paper analytical devices for quantitative point-of-care aptamer-based assays

Haiyan Fu[a,*], Juanhua Yang[b], Lin Guo[b], Jinfang Nie[b,*] Qiaobo Yin[a], Lang Zhang[b], Yun Zhang[b,*]

[a]*The Modernization Engineering Technology Research Center of Ethnic Minority Medicine of Hubei Province, School of Pharmaceutical Sciences, South-Central University for Nationalities, Wuhan 430074, P. R. China.*

[b]*Guangxi Key Laboratory of Electrochemical and Magnetochemical Function Materials, College of Chemistry and Bioengineering, Guilin University of Technology, Guilin 541004, P. R. China.*

fuhaiyan@mail.scuec.edu.cn (H. Fu)

Niejinfang@glut.edu.cn (J. Nie)

zy@glut.edu.cn (Y. Zhang)

*Corresponding author.

Abstract

In this article, we describe a facile method named as Rubik's Cube stamping (RCS) for equipment-free fabrication of microfluidic paper-based analytical devices (μPADs). RCS is inspired by the worldwide ubiquitous RC toy and requires no specialized electric equipment other than a classical six-faced RC that is assembled with home-made small

iron components. It can pattern various rosin microstructures in paper simply by either using different functional faces of the modified RC or applying its internal pivot mechanism to adjust the components' patterning forms on one functional face. Such a versatile stamping method is quite simple and inexpensive, and thus holds potential for producing rosin-patterned μPADs by untrained users in resource-limited environments such as small laboratories and private clinics, or even at home and in the field. Moreover, a set of one-channel devices are fabricted to design a point-of-care aptamer-based assay with near sample-in–answer-out capability that integrates enzymatic reactions for robust yet efficient signal amplification and a personal glucometer for portable, user-friendly, rapid and quantitative readout. Its utility is well demonstrated with the sensitive and specific detection of adenosine as a model target in buffer samples and undiluted human urine within several minutes. With the advantages of low cost, simplicity, portability, rapidity, and aptamer variety, this general point-of-care assay system reported here may find broad applications including home healthcare, field-based environmental monitoring or food analysis and emergency situations.

Keywords: Point-of-care testing; Biosensor; Aptamer; Paper-based bioanalysis; Glucose meter

1. Introduction

It is crucial to develop facile assays for quantitative detection of a broad range of targets in various resource-poor settings especially in the developing world where improving healthcare, environmental protection and food safety is becoming increasingly important (Lin et al., 2014; Tokel et al., 2014; Zhu et al., 2014). The most ideal assay should be affordable, sensitive,

specific, user-friendly, rapid and robust, equipment-free and deliverable to the end user to satisfy the ASSURED standard proposed by the World Health Organization (Urdea et al., 2006). In this context, considerable effort has been devoted to the design of multifarious point-of-care assays to meet these ASSURED requirements as much as possible, such as lateral flow test strips (Li et al., 2016c), colorimetric systems (Guo et al., 2013; Nie et al., 2016), microfluidic chips (Gervais et al., 2011; Segerink and Eijkel, 2014), and recently emerged patterned paper platforms, mostly known as the microfluidic paper-based analytical devices (μPADs) (Cate et al., 2015; Yang et al., 2017; Yamada et al., 2015).

By comparison, the cencept of μPADs, which can offer the advantages inherited from both the lateral flow test strips and the conventional microfluidic chips, has gained ever-growing attention (Ahmed et al., 2016; Desmet et al., 2016; Ellerbee et al., 2009; Garcia et al., 2014; Hu et al., 2014; Lin et al., 2016; Meredith et al., 2016; Mettakoonpitak et al., 2016; Wu et al., 2015a; Xi et al., 2016). Key among their attractive features include cost-effective paper substrates, low dosages of reagents and samples, rapid reactions in capillary action-driven liquid flow, ease of device storage/transport/use, portability and multiplexing capacity. As a result, the last decade has witnessed fast progress in the development of a variety of paper-based assays for detection of diverse analytes of interest including ions (Ge et al., 2016; Sjöberg et al., 2016; Zhang et al., 2015), small molecules (Li et al., 2016b; Wei et al., 2015; Zhang et al., 2016b; Zhang et al., 2014), DNAs (Li et al., 2016a; Li and Scida, 2015; Scida et al., 2013), proteins (Li et al., 2016a; Sechi et al., 2013; Yang et al., 2014; Zhao et al., 2016) and cancer cells (Wu et al., 2015b; Novell et al., 2014), implying their great potential in broad applications ranging from medical diagnosis, environmental monitoring to food analysis. However, the μPADs were generally fabricated with the aid of benchtop electric equipment such as lithography machines, printers and lasers and/or heating unit (Yamada et al., 2015; Yetisen et al., 2013; Xia et al., 2016). Moreover, most quantitative assays might

still suffer from the disadvantages of multistep target binding reactions and/or data processings (Nilghaz et al., 2016; Zhang et al., 2015; Zhang et al., 2016b). These may add the total cost and complexity of the devices and the analytical processes to many existing paper-based assays. Thus, the need might still remain for alternative fabrication strategies and point-of-care assays with (near) sample-in–answer-out capability to be widely implemented by untrained users at minimum cost even at home and in the field.

In this work, we describe a complementary quantitative point-of-care assay on the μPADs that are created by only using a Rubik's Cube (RC) rather than any electric equipment. RC, originally called Magic Cube, is a worldwide ubiquitous 3D toy invented in 1974 by Hungarian sculptor and professor of architecture Ernő Rubik. Each face of a classic six-faced RC consists of nine solid elements. An internal pivot mechanism enables each face and element to turn independently. Some efforts have been dedicated to RC-inspired watermark encryption technology (Abitha et al., 2016; Yen and Lin, 2010) and metal nanocluster preparation (Yang et al., 2017). Encouraged by the RC's interesting pattern adjustability, a new method is proposed herein for equipment-free μPAD fabrication, which we call RC stamping (RCS). As schematically shown in Fig. 1, five faces of a classic six-faced RC are separately assembled with five groups of homemade small iron components with specific patterns to offer fabrication or adjustment functions. The bare sixth face acts as the supporting face when the modified RC is not used. The RCS for paper patterning only involves two operations: (1) immersing of the patterned metal components on one RC face in a rosin solution and (2) stamping of the rosin layer-coated components on paper surface. During the stamping process, the rosin solution can penetrate through the paper body. After

rapid evaporation of the low-boiling solvent (ethyl alcohol), the rosin remaining in paper will form hydrophobic barriers to direct hydrophilic flow channels or independent test zones.

We then use as-prepared one-channel μPADs to develop a point-of-care aptamer-based assay with near sample-in–answer-out capability. This assay integrates enzymatic reactions for robust yet efficient signal amplification and a simple and low-cost personal glucometer for portable, rapid and quantitative readout. Adenosine is chosen as the initial modle target for the study because it is a vital cofactor in many biological processes such as kidney function; its renal levels in urine higher than normal (micromolar) range are characteristic of diseases (Liu et al., 2012). Most of reported aptamer-based adenosine assays typically transduce the recognition chemistry using fluorescence (Dave and Liu, 2012; Helwa et al., 2012; Huang and Liu, 2010; Liu et al., 2013; Song et al., 2012; Xiang et al., 2009; Xu and Lu, 2010), absorbance (Liu et al., 2006; Liu and Lu, 2004; Zhao et al., 2008), or luminescence (Li et al., 2012; Liu et al., 2007) readers, but these measurements would limit their point-of-use applications. Personal glucometers are one family of point-of-care testing devices among the most successful and widely-used sensors around the world. They are cheap, portable, user-friendly and enable quantitative detection of glucose levels in several seconds. Some novel assay methods have been recently proposed for the detection of several non-glucose targets by using the glucometers as quantitative readers (Wang et al., 2016; Yan et al., 2013; Zhang et al., 2016a). So far, however, there are few reports of (near) sample-in–answer-out aptamer-based assays carried out on μPADs with glucometer readout. The results demonstrate that this point-of-care assay system allows for simple, low-cost, sensitive, specific and portable detection of adenosine in buffer samples and undiluted human urine within several minutes.

2. Materials and methods

2.1. Materials and apparatus

Amylose, α-amylase, β-amylase, γ-amylase (also called glucoamylase), streptavidin (from *Streptomyces avidinii*, >13 U/mg), glutaraldehyde and dimethyl sulfoxide were obtained from Sigma-Aldrich. Amine-coated SiO_2 microbeads (MBs, ~ 10 μm in diameter) were the products of Tianjin BaseLineChrom Tech Research Centre (Tianjin, China). The 24-unit ethylene glycol functionalized with succinimidyl and maleimido ends was bought from Thermo Scientific. Adenosine, cytidine, uridine, lysine and bovine serum albumin were the products of Sangon Biotechnology Co. Ltd. (Shanghai, China). All oligonucleotides were ordered from Takara Biotechnology Co., Ltd. (Dalian, China). Their thermodynamic parameters were calculated by using bioinformatics software (Zuker, 2003). The sequences of the oligonucleotides (from 5′ to 3′) were listed as follows (Liu et al., 2012): aptamer strand, TTT TTT ACT CAT CTG TGA AGA GA*A CCT GGG GGA GTA TTG CGG AGG AAG GT* (the sequence for binding adenosine is in italics); capture DNA strand 1 (for glucoamylase conjugation), biotin-$(CH_2)_6$-AAA AAA AAA AAA CCC AGG TTC TCT; and capture DNA strand 2 (for MB conjugation), TCA CAG ATG AGT AAA AAA AAA AAA-$(CH_2)_6$-NH_2. Human urine samples were collected from health volunteers. Rosin with a melting point of 172 °C was from Sinopharm Chemical Reagent Co., Ltd (Shanghai, China). Aqueous red ink was from Guilin Fuxuan Chemical Product Co., Ltd. (Guilin, China). All other chemicals were of analytical grade and were used as received. Unless otherwise specified, all solutions were prepared with ultrapure water (with a specific resistivity >18.2 MΩ·cm) from an ultrapure water system (UPS-II-20L) provided by Chengdu Yuechun Technology Co., Ltd. (Chengdu, China). Phosphate-buffered saline (PBS, 10 mM, pH 7) solution containing 50 mM NaCl was prepared with Na_2HPO_4 and KH_2PO_4.

Filter paper made from pure cellulose was from Hangzhou Xinhua Paper Industry Co., Ltd. (Hangzhou, China). Filter paper is used here as one example of practice for μPAD fabrication, but other types of paper substrates or porous films such as nitrocellulose

membrane are also suitable. Disposable one-time graduated Pasteur pipets were the products of Shanghai JingAn Biological Technology Co., Ltd. (Shanghai, China). Five groups of iron components (2 mm in thickness) with specific patterns (~ $5.8) were obtained from Wuhan Chutian Laser Group Co., Ltd. (Wuhan, China). A classic six-faced 3D Rubik's Cube (RC) (~ $2.6) was from Thumb Park Puzzle Toy Co., Ltd (Beijing, China). Home-use personal glucometer (Omron, HGM-114) was bought from Daertai Enterprise Co, Ltd (Tianjin, China).

2.2. Patterning of paper with rosin

The principle and process behind the RCS method for μPAD fabrication are schematically shown in Fig. 1. Before the paper patterning, five faces of the six-faced RC were assembled with five groups of different iron components separately by using two-component epoxy resin adhesive, according to the five kinds of pre-designed complete patterns (Fig. 1, bottom). For the generation of a rosin-patterned device such as an eight-channel μPAD, the patterned metal components of the RC's eight-channel face (i.e., the face 2) were first immersed in a rosin solution (600 mg/mL) in ethyl alcohol for several seconds. The depth of the rosin solution should be lower than the height of the components (i.e., 5 mm). The patterned iron components coated with a rosin layer and the RC body were then taken out and in turn used synergistically as a "stamp" to print a corresponding pattern of rosin microstrcutures into paper (Fig. 1, top right). The resultant patterned paper was subsequently left at room temperature to evaporate the solvent in the rosion pattern. The modified RC is reusable because the iron components have good mechanical strength. Various rosin-patterned μPADs could be created by either using different fabrication faces on the RC or simply adjusting the iron components on the blocking face to re-arrange the patterns of the metal components on

the four basic fabrication faces. Note that it is necessary to avoid the exposure of the rosin-patterned μPADs in the organic solvents which can dissolve the rosin patterns.

2.3. Preparation of glucoamylase-labeled DNA

The glucoamylase was first labeled with streptavidin: 4 μL of 250 mM 24-unit ethylene glycol functionalized with succinimidyl and maleimido ends in dry dimethyl sulfoxide was mixed with 1 mL of 6 mg/mL streptavidin in PBS for 0.5 h at room temperature (ca. 25 °C). After the reaction solution was dialyzed to remove excess cross-linker and further diluted with the buffer to its original volume, 20 mg glucoamylase was added and incubated at 4 °C overnight. Then, 10 μM biotinylated capture DNA strand 1 was added to the above mixture solution for 24 h incubation at 4 °C, resulting in the formation of glucoamylase-labeled DNA conjugates.

2.4. Preparation of biofunctionalized MB probes

Capture DNA strand 2 was first immobilized onto the MB surface. In biref, 20 μL of 0.5% (w/v) amine-coated MB suspension was mixed with 5 mL of 5% (w/v) glutaraldehyde solution in water. After the mixture was incubated for 3 h at room temperature, the MBs were isolated by centrifugation and washed three times with PBS to remove un-reacted glutaraldehyde molecules. The aldehyde-activated MBs were then dispersed in 200 μL of 1 μM capture DNA strand 2 solution. Another 3 h incubation later, 1 mL of 1 mM lysine solution was used to block the remaining aldehyde groups on the MBs. After centrifugation separation and washings, the DNA strand 2-MB bioconjugates were re-suspended in 40 μL of PBS buffer. Next, a 40 μL solution containing 10 μM glucoamylase-labeled DNA strand 1 and 12 μM aptamer strand was mixed with the resulting solution for incubation at 4 °C overnight. After the as-prepared MB probes

functionalized with aptamer and glucoamylase were isolated by centrifugation and washed with buffer, they were re-suspended in 200 μL of PBS (containing 10 mg/mL bovine serum albumin) and stored at 4 °C for further use.

2.5. Fabrication and reagent loading of one-channel μPADs

A set of one-channel rosin-patterned μPADs were fabricated by the RCS method to design the point-of-care aptamer-based adenosine assays (as depicted in Fig. 3). This one-channel pattern was formed by re-arranging the metal components on the RC's fabrication face 1 using the blocking face. Each device consists of "FOUR" interconnected functional zones: zone a for sample introduction, zone b for loading of MB probes, zone c for amylose immobilization, and zone d for buffer addition (for glucometer measurement). Before the detection reagent immobilization, the hydrophilic zones of every μPAD were pretreated by incubating them in a mixture of 10 mg/mL bovine serum albumin and 0.05% (v/v) Tween-20 in PBS and allowing the zones to air-dry. Then, 0.8 μL of 0.05% (w/v) MB probes and 3 μL of amylose solution (30 mg/mL) was dropcast in the zones b and c, respectively, and dried in air. The reagent-loaded μPADs freshly prepared were encapsulated separately in glossy, transparent plastic bags and stored together with hygroscopic agents in dry place (away from light) at room temperature until used. Each reagent-loaded μPAD costs ~ $0.0072.

2.6. Adenosine assay procedures

In a typical adenosine assay, one drop (ca. 20 μL) of buffer sample or human urine sample was added onto the zone a in a reagent-immobilized device using a graduated Pasteur pipet. The liquid would flow rapidly in the hydrophilic paper channel via capillary action. When it filled the zone d (within about 4 min), another drop (ca. 10 μL) of buffer was introduced in

the zone d to suspend possible glucose products for glucometer measurement. It took totally about 6 min to complete the whole adenosine assay.

The specificity experiments for cytidine and uridine were carried out in the same way. All the experiments were performed at room temperature (~ 25 °C).

3. Results and discussion

3.1. Equipment-free fabrication of μPADs via the Rubik's Cube stamping

Inspired by the worldwide ubiquitous 3D RC toy, a new method, namely the RCS method is reported herein for the fabrication of μPADs without using specialized electric equipment (as depicted in Fig. 1). The RCS only uses a classic six-faced RC. The RC's five faces are separately decorated with five groups of iron components with predesigned patterns to offer fabrication or adjustment (blocking) functions, while the sixth face is bare and used as the supporting face when the decorated RC is not used. At least four types of rosin-patterned devices, i.e., the four-, eight-, and sixteen-channel μPADs and a 3×3 circular microzone array designed in this study, can be fabricated directly by using the four basic fabrication faces of the modified RC (Fig. 1, bottom, images 1-4). In addition, twelve more types of μPADs can be obtained by simply adjusting the blocking face once to re-arrange the component patterns on the basic fabrication faces (Fig. S1 and Videos S1-24 in Supplementary Data). It is not recommended to perform more (complex) adjustments to realize more specific arrangements of the small components for paper patterning, unless absolutely necessary..

In the RCS method, the iron was chosen as the component material because it is very cheap and has good mechanical strength. The rosin is a kind of quite inexpensive industrial raw material, has a melting point higher than 170 °C, and is soluble in nontoxic organic solvent such as ethyl alcohol; thus it is the ideal "green ink" for paper patterning even at home or in the field. Moreover, it was experimentally found that the rosin concentration had a big

influence on the formation of repeatable patterns in paper body (Fig. S2, Supplementary Data). Stable rosin patterns were achieved when the applied rosin concentration was higher than 600 mg/mL, which was thereby recommended for all of the experiments. The fabrication resolution of the rosin-patterned hydrophilic channel in the chosen type of paper (filter paper) was also characterized. As shown in Fig. S3 (Supplementary Data), the smallest width of paper channel with a relative standard deviation (RSD) less than 10% was estimated to be ~ 2.5 mm, suggesting the acceptable fabrication resolution and reproducibility of the RCS method.

Fig. 2A displayed the images of the rosin-patterned four-, eight-, and sixteen-channel μPADs, a 3 × 3 circular microzone array and a foursquare microzone fabricated from the corresponding five function faces of the decorated RC (Fig. 1, bottom). One can clearly see that the RCS method allowed for the production of well-defined rosin patterns in the paper. After fast evaporation of the solvent (in several seconds), the rosin microstructures remained in the patterns further acted well as hydrophobic barriers to direct the flowing of aqueous red ink solution, for example in the eight-channel μPAD (Fig. 2A, image b), indicating that rosin liquid had penetrated across the thickness of the paper body during the RC stamping process. As such, the rosin-free hydrophilic independent paper channels were defined by the hydrophobic rosin-contained regions. Moreover, the RCS has an interesting intrinsic fabrication adjustability inherited from the RC body. That is, diversified μPADs to meet particular requirements can be created by adjusting the iron components on the blocking face (face 5) to re-form the corresponding patterns of the metal components of the same group on any fabrication face. For instance, other four kinds of congenetic μPADs, i.e., the one-, three-,

five-, and seven-channel μPADs were produced after the replacement of seven, five, two and one component(s) on the eight-channel RC face (face 2) with the same number of components on the blocking face, respectively (Fig. 2B).

The stability study additionally showed that no significant shape changes were observed in the rosin patterns in the as-prepared μPADs when they were kept in an oven of 60 °C and 45 °C for 24 h and 1 month, respectively. In other words, the rosin microstructures in the paper body did not melt at the elevated temperatures due to its melting point of ca. 172 °C. As a consequence, the rosin-patterned μPADs produced by the RCS method could be stably stored under 60 °C, which is sufficient for normal use in common non-laboratory environments.

3.2 Point-of-care aptamer-based assay with glucometer for portable detection of adenosine

To test the analytical utility of the rosin-patterned μPADs, a set of one-channel devices were fabricated to design a near sample-in–answer-out aptamer-based assay with portable glucometer readout for point-of-care detection of adenosine model target (as depicted in Fig. 3). The one-channel pattern was obtained by adjusting the iron components on the fabrication face 1 of the modified RC'swith the blocking face. Each one-channel μPAD consists of "FOUR" interconnected functional zones a-d that were used for the sample introduction, loading of ~ 10 μm diameter MB probes coated with glucoamylase and adenosine-specific aptamer, amylose immobilization and buffer addition (to suspend possible glucose products for glucometer readout), respectively. After the immobilization of MB probes and amylose, every device was encapsulated in a glossy and transparent plastic bag and stored together with hygroscopic agents in dry place away from light. In the assay, when the sample solution

added in the zone a flows through the zone b via capillary action, the aptamers selectively bind the adenosine molecules to form target−aptamer complexes, resulting in in-situ release of the glucoamylase from the MB surface. The released enzyme then runs into zone c to catalyze the hydrolysis of amylose to generate a large number of glucose. The glucose products in turn flow into the zone d to be further suspended in the buffer for quantitative readout by the glucometer. No glucose would be produced in the zone d in the absence of analyte in the sample. The whole near sample-in–answer-out analytical processes can be finished within several minutes.

In our assay, the analyte concentration is proportional to the amount of glucose that positively depends on the level of released enzyme and its glucose-producing efficiency. As such, the use of amylase enzyme with greater glucose producion should lead to the enhanced detection sensitivity. We thus optimized the enzyme type. In general, there are three types of amylase, i.e., α-amylase, β-amylase, and γ-amylase (also called glucoamylase). To compare their glucose-producing efficiencies, these three types of amylase enzymes were applied to hydrolyze three amylose solutions with the same concentrations over the same period, followed by measurements of the final glucose yields with the glucometer. As shown in Fig. 4A, average readings of 3.2 and 10.9 mM were obtained for α-amylase and γ-amylase, respectively, but no detectable reading was observed for β-amylase. The data indicates that the γ-amylase, namely the glucoamylase possesses the highest glucose-producing efficiency, which is therefore considered to be the ideal enzyme to use in our method.

Next, the feasibility of releasing the glucoamylase from the MB probe via the adenosine-aptamer binding to hydrolyze the amylose to produce glucose along the hydrophilic paper

channel was studied. Several reagent-immobilized μPADs were adopted to analyse a 400 μM adenosine sample, comparing with the result of assaying a control (blank) sample (i.e., the PBS buffer without analyte). The glucose possibly produced in the zones c and d of each μPAD was separately collected for glucometer readout. As shown in Fig. 4B, for the control sample (black bars), no detectable glucometer signal was obtained for the zone c of the μPAD used (black bars) and a very low average reading was measured for its zone d, which indirectly reflected the stable immobilization of the micron-sized MB probes in zone b (with ignorable displacement into zone c) after exposure to buffer solution. On the other hand, as expected, a high average reading up to 21.7 mM for the zone d in the adenosine assay was achieved (Fig. 4B, red bar). A low glucometer signal (2.5 mM) was also observed for the zone c in this case. The data confirms that the target-aptamer binding could successfully release the enzyme (from the MB surface) that sequently digested its substrate in zone c to produce glucose but most of which finally ran into the zone d. Moreover, similar glucometer signals were measured from the zones d of the μPADs used for the analysis of several adenosine samples at the same levels under different temperatures and humidities (data not shown). This may be presumably attributed to the fact that the rapid near sample-in–answer-out analytical procedures (similar to that of the lateral flow test strips) could minimize the influences of the two environmental factors.

Since the dosages of the glucoamylase-coated MB probes and amylose are also strongly related to the glucose production, we further optimized the two factors. Greater amounts of MB probes and the substrate loaded in the μPAD should be beneficial to increased glucose production to ensure higher sensitivity of the new system. However, the capacities of zones b and c for the two reagents' loading are limited. Too high concentrations of MB probes and amylose molecules could even fill fully the two hydrophilic regions to block the liquid flow in the device. To optimize their dosages, a set of μPADs loaded with different levels of 0.05%

(w/v) MB probe (0.2 − 1.2 μL) and amylose (10 − 50 mg/mL) were used to assay adenosine samples with the same concentration. As shown in Figs. S4 and 5 (Supplementary Data), the highest glucometer signals were obtained at 0.8 μL of 0.05% (w/v) MB probe and 30 mg/mL amylose, which were thus chosen as the optimal dosages in subsequent experiments.

After system optimization, the proposed method was applied to assay a series of adenosine samples with varying concentrations in PBS buffer. Each sample was tested with three measurements in parallel. As shown in Fig. 5A, the glucometer signal increased with

increasing adenosine concentration, indicating the analyte level-controlled glucose generation. More importantly, the glucometer signal was proportional to the concentration of adenosine in the range of 0 to 900 μM, establishing the quantitative detection capability of our assay. A limit of detection for the analyte was determined to be ca. 5.7 μM, based on 3σ/slope, where σ represents the standard deviation of the blank (control) samples. In comparison with some typical quantitative aptamer-based adenosine assays previously reported with fluorescence (Dave and Liu, 2012; Helwa et al., 2012; Huang and Liu, 2010; Liu et al., 2013; Song et al., 2012; Xiang et al., 2009; Xu and Lu, 2010), absorbance (Liu et al., 2006; Liu and Lu, 2004; Zhao et al., 2008), luminescence (Li et al., 2012; Liu et al., 2007), electrochemistry (Zhang et al., 2008; Liu et al., 2012; Wu et al., 2007), nuclear magnetic resonance (Yigit et al., 2007), surface plasmon resonance (Wang et al., 2008), or insturment-free (Zhang et al., 2016b) measurement, this near sample-in–answer-out μPAD-based strategy with glucometer readout could offer several advantages in that it is low-cost and rapid, requires no specialized skills to achieve comparable or even better sensitivity, and allows for point-of-care applications (Table S1 in Supplementary Data).

Moreover, the selectivity of this new assay system was investigated by assaying cytidine and uridine that belong to the nucleofaces family as negative controls. Guanosine was not tested because of its low solubility in PBS buffer at room temperature (Liu et al., 2006). One can clearly find from Fig. 5B that as for either cytidine or uridine, the glucometer signal obtained could be negligible. In contrast, only 240 μM adenosine produced an average reading that was almost 56-fold larger than that of the other two types of nucleofaces at 2 mM. This result implies that the prepared μPADs retained the aptamer's excellent binding selectivity towards the target, adenosine.

To further assess the accuracy and practicability of the proposed method, detection of adenosine in human urine was performed. Different concentrations of standard solutions of adenosine were added into undiluted human urine and analysed according to the general procedures. The results were summarized in Table S2 (Supplementary Data). As presented in Table S2, the obtained recovery results ranged from 98.9 to 109.4% and the RSDs were in the range of 6.2 – 9.6% (n=10), thus validating the acceptable recovery and practicability of the new assay for detection of adenosine in complex matrices such as body fluids. Its satisfactory practicality should be due to that the aptamer could keep its highly specific molecular recognition capacity for the adenosine target in the human urine samples. Moreover, as the paper channel itsself has separation and purification properties, it could additionally reduce the effects of interferences in such complex matrices to some extent.

The acceptable shelf life of our reagent-loaded μPADs is another consideration if they would be used especially for public or in-field applications. As shown in Fig. S5 (Supplementary Data), after storage (in dry place away from light) for 3 months, these reagent-loaded μPADs performed as well as freshly prepared devices, establishing that they were robust, stable and reliable. More satisfactory storage stability could be expected if these

devices were vacuum packed in impermeable non-transparent plastic envelopes to minimize reagent deactivation and possible contamination.

4. Conclusion

We have developed a facile method termed RCS (Rubik's Cube stamping) for low-cost and adjustable fabrication of μPADs. The RCS requires no external electric equipment and toxic materials and is sufficiently simple to be performed by nontechnical personnel. It thus represents a promising addition to the existing arsenal for the μPAD production especially in various resource-poor settings (e.g., small laboratories and private clinics) or even at home and in the field. The utility of the as-prepared μPADs was further demonstrated with the development of a point-of-care aptamer-based assay with near sample-in–answer-out capability that integrated enzymatic reactions for signal amplification with a ubiquitous glucometer for inexpensive, rapid, portable, user-friendly and quantitative readout. Although we used an adenosine aptamer for this initial proof-of-concept study, a variety of aptamers binding a broad range of other targets that are either available or could be obtained through the SELEX (systematic evolution of ligands by exponential enrichment) technique (Tan et al., 2013) could also be adopted in the same sensing system. In view of the low cost, portability, rapid detection, user-friendliness, and wide availability of μPADs and glucometers, we believe that the assay system described herein will prove promising for wide applications such as point-of-care diagnosis and in-filed analysis.

Acknowledgment

The authors gratefully acknowledge the financial support from National Science Foundation of China (21576297, 21565012, 21365009 and 21205021) and Project of High

Level Innovation Team/Outstanding Scholar and Key Laboratory of Food Safety and Detection in Guangxi Colleges and Universities (2015GXNSFFA139005).

References

Abitha, K.A., Pradeep, K.B., 2016. Procedia Technol. 24, 782–789.

Ahmed, S., Bui, M.N., Abbas, A. 2016. Biosens. Bioelectron. 77, 249–263.

Cate, M.D., Adkins, J.A., Mettakoonpitak, J., Henry, C.S., 2015. Anal. Chem. 87, 19–41.

Dave, N., Liu, J.W., 2012. Chem. Commun. 48, 3718–3720.

Desmet, C., Marquette, C.A., Blum, L.J., Doumèche, B., 2016. Biosens. Bioelectron. 76, 145–163.

Ellerbee, A.K., Phillips, S.T., Siegel, A.C., Mirica, K.A., Martinez, A.W., Striehl, P., Jain, N., Prentiss, M., Whitesides, G.M., 2009. Anal. Chem. 81, 8447–8452.

Garcia, P.deT., Cardoso, T.M.G., Garcia, C.D., Carrilho, E., Coltro, W.K.T., 2014. RSC Adv. 4, 37637–37644.

Ge, S.J., Wu, K.Q., Zhang, Y., Yan, M., Yu, J.H., 2016. Biosens. Bioelectron. 80, 215–221.

Gervais, L., De Rooij, N., Delamarche, E., 2011. Adv. Mater. 2011, 23, H151–H176.

Guo, L.H., Xu, Y., Ferhan, A.R., Chen, G.N., Kim, D., 2013. J. Am. Chem. Soc. 135, 12338–12345.

Helwa, Y., Dave, N., Froidevaux, R., Samadi, A., Liu, J.W., 2012. ACS Appl. Mater. Interfaces 4, 2228−2233.

Hu, J., Wang, S.Q., Wang, L., Li, F., Pingguan-Murphy, B., Lu, T.J., Xu, F., 2014. Biosens. Bioelectron. 54, 585–597.

Huang, P.J., Liu, J.W., 2010. Anal. Chem. 82, 4020–4026.

Li, H., Fang, X.E., Cao, H.M., Kong, J.L., 2016a. Biosens. Bioelectron. 80, 79–83.

Li, J., Macdonald, J., 2016b. Biosens. Bioelectron. 83, 177–192.

Li, L., Zhang, Y., Zhang, L.N., Ge, S.G., Liu, H.Y., Ren, N., Yan, M., Yu, J.H., 2016c. Anal. Chem. 88, 5369–5377.

Li, L.L., Ge, P.H., Selvin, P.R., Lu, Y., 2012. Anal. Chem. 84, 7852−7856.

Li, X., Scida, K., Crooks, R.M., 2015. Anal. Chem. 87, 9009–9015.

Lin, Y., Gritsenko, D., Feng, S.L., Teh, Y.C., Lu, X. N., Xu, J., 2016. Biosens. Bioelectron. 83, 256–266.

Liu, B.W., Du, D., Hua, X., Yu, X.Y., Lin, Y.H., 2014. Electroanalysis 26, 1214–1223.

Liu, H., Xiang, Y., Lu, Y.R., Crooks, M., 2012. Angew. Chem. Int. Ed. 51, 6925–6928.

Liu, J. B., Liu, Y., Yang, X.H., Wang, K.M., Wang, Q., Shi, H., Li, L., 2013. Anal. Chem. 85, 11121–11128.

Liu, J.W., Lee, J.H., Lu, Y., 2007. Anal. Chem. 79, 4120–4125.

Liu, J.W., Lu, Y., 2004. Anal. Chem. 76, 1627–1632.

Liu, J.W., Mazumdar, D., Lu, Y., 2006. Angew. Chem. Int. Ed. 45, 7955–7959.

Nie, J.F, Brown, T., Zhang, Y., 2016. Chem. Commun. 52, 7454–7457.

Nilghaz, A., Guan, L. Y., Tan, W.R., Shen, W., 2016. ACS Sens. 1, 1382−1393.

Novell, M., Guinovart, T., Blondeau, P., Xavier Rius, F., Andrade, F.J., 2014. Lab Chip 14, 1308–1314.

Meredith, N.A., Quinn, C., Cate, D.M., Reilly, T.H., Charles, J.V., Henry, S., 2016. Analyst, 2016,141, 1874–1887.

Mettakoonpitak, J., Boehle, K., Nantaphol, S., Teengam, P., Adkins, J.A., Srisa-Art, M., Henry, C.S., 2016. Electroanalysis 28, 1420–1436.

Scida, K., Li, B.L., Ellington, A.D. Crooks, R.M., 2013. Anal. Chem. 85, 9713–9720.

Sechi, D., Greer, B., Johnsonand, J., Hashemi, N., 2013. Anal. Chem. 85, 10733–10737.

Segerink, L.I., Eijkel, J.C.T., 2014. Lab Chip 14, 3201–3205.

Sjöberg, P., Määttänen, A., Vanamo, U., Novell, M., Ihalainen, P., Andrade, F.J., Bobacka, J., Peltonen, J., 2016. Sens. Actuat. B: Chem. 224, 325–332.

Song, P.S., Xiang, Y., Xing, H., Zhou, Z.J., Tong, A.J., Lu, Y., 2012. Anal Chem. 84, 2916–2922.

Tan, W.H., Donovan, M.J., Jiang, J.H., 2013. Chem. Rev. 113, 2842–2862.

Tokel, O., Inci, F., Demirci, U., 2014. Chem. Rev. 114, 5728−5752.

Urdea, M., Penny, L.A., Olmsted, S.S., Giovanni, M.Y., Kaspar, P., Shepherd, A., Wilson, P., Dahl, C.A., Buchsbaum, S., Moeller, G., Burgess, D.C.H., 2006. Nature 444 (suppl. 1), 73.

Wang, C.C., Hennek, J.W., Ainla, A., Kumar, A.A., Lan, W.J., Im, J., Smith, B.S., Zhao, M. X., Whitesides, G.M., 2016. Anal. Chem. 88, 6326−6333.

Wang, J.L., Zhou, H.S., 2008. Anal. Chem. 80, 7174–7178.

Wei, X.F., Tian, T., Jia, S.S., Zhu, Z., Ma, Y.L., Sun, J.J., Lin, Z.Y., James Yang, C.Y., 2015. Anal. Chem. 87, 4275–4282.

Wu, K.Q., Zhang, Y., Wang, Y.H., Ge, S.G., Yan, M., Yu, J.H., Song, X.R., 2015a. ACS Appl. Mater. Interfaces, 7, 24330–24337.

Wu, L.D., Ma, C., Ge, L., Kong, Q.K., Yan, M., Ge, S.G., Yu, J.H., 2015b. Biosens. Bioelectron. 63, 450–457.

Wu, Z.S., Guo, M.M., Zhang, S.B., Chen, C.R., Jiang, J.H., Shen, G.L., Yu, R.,Q., 2007. Anal. Chem. 79, 2933–2939.

Xiang, Y., Tong, A.J., Lu, Y., 2009. J. Am. Chem. Soc. 131, 15352–15357.

Xu, W.C., Lu, Y., 2010. Anal. Chem. 82, 574–578.

Yan, L., Zhu, Z., Zou, Y., Huang, Y.S., Liu, D.W., Jia, S.S., Xu, D.M., Wu, M., Zhou, Y., Zhou, S., James Yang, C.Y., 2013. J. Am. Chem. Soc. 135, 3748−3751.

Yang, F., Zuo, X.L., Li, Z.H., Deng, W.P., Shi, J.Y., Zhang, G.J., Huang, Q., Song, S.P., Fan, C.H., 2014. Adv. Mater. 26, 4671–4676.

Yang, H.Y., Yan, J.Z., Wang, Y., Su, H.F., Gell, L., Zhao, X.J., Xu, C.F., Teo, B.K., Hannu Häkkinen, H., Zheng, N.F., 2017. J. Am. Chem. Soc., 139, 31–34.

Yang, Y.Y., Noviana, E., Nguyen, M.P., Geiss, B.J., Dandy, D.S., Henry, C.S., 2017. Anal. Chem. 89, 71−91.

Yamada, K., Henares, T.G., Suzuki, K., Citterio, D., 2015. Angew. Chem. Int. Ed. 54, 5294–5310.

Yen, E., Lin, L., H., 2010. Expert Syst. Appl. 37, 4033–4039.

Yetisen, A.K., Akram, M.S., Lowe, C.R., 2013. Lab Chip 13, 2210–2251.

Yigit, M.V., Mazumdar, D., Kim, H., Lee, J.H., Odintsov, B., Lu, Y., 2007. ChemBioChem 8, 1675–1678.

Xi, Y.Y., Si, J., Li, Z.Y., 2016. Biosens. Bioelectron. 77, 774–789

Xia, Y.Y., Si, J., Li, Z.Y., 2016. Biosens. Bioelectron. 77, 774–789.

Zhang, J.J., Shen, Z., Xiang, Y., Lu, Y., 2016a. ACS Sens. 1, 1091–1096.

Zhang, S.S., Xia, J.P., Li, X.M., 2008. Anal. Chem. 80, 8382–8388.

Zhang, Y., Fan, J.L., Nie, J.F., Le, S.W., Zhu, W.Y., Gao, D., Yang, J.N., Zhang, S.B., Li, J.P., 2015. Biosens. Bioelectron. 73, 13–18.

Zhang, Y., Gao, D., Fan, J.L., Nie, J.F., Le, S.W., Zhu, W.Y., Yang, J.N., Li, J.P., 2016b. Biosens. Bioelectron. 78, 538–546.

Zhang, Y., Zhou, C.B., Nie, J.F., Le, S.W., Qin, Q., Liu, F., Li, Y.P., Li, J.P., 2014. Anal. Chem. 86, 2005–2012.

Zhao, M., Li, H.F., Liu, W., Guo, Y.M., Chu, W.R., 2016. Biosens. Bioelectron. 79, 581–588.

Zhao, W.A., Chiuman, W., Lam, J.C.F., McManus, S.A., Chen, W., Cui, Y.G., Pelton, R., Brook, M.A., Li, Y.F., 2008. J. Am. Chem. Soc. 130, 3610–3618.

Zhu, Z., Guan, Z. C., Jia, S.S., Lei, Z.C., Lin, S.C., Zhang, H.M., Ma, Y.L., Tian, Z.Q., James Yang, C.Y., 2014. Angew. Chem., Int. Ed., 2014, 53, 12503−12507.

Zuker, M., 2003. Nucleic Acids Res. 31, 3406–3415.

Figure captions

Fig. 1 Schematic of the proposed RCS method for equipment-free stamping fabrication of a rosin-patterned eight-channel μPAD. Five faces of a classic six-faced RC (Rubik's Cube) are assembled separately with five groups of small iron components to offer specific fabrication or adjustment functions, while the bare sixth face acts as the supporting face when the assembled RC is not used.

Fig. 2 (A) Images of the rosin-patterned four-, eight- and sixteen-channel μPADs, a 3 × 3 circular microzone array, and a square microzone created from the basic fabrication and adjustment faces of the assembled RC (with corresponding patterns shown in **Fig. 1**). The rosin-free central regions of the eight-channel μPAD had been wetted with aqueous red ink. (B) Images of the rosin-patterned one-, three-, five- and seven-channel μPADs fabricated by using the RC's blocking face (face 5) to adjust the patterns of the iron components on its face 2 used for the eight-channel μPAD shown in (A). Each of the scale bars is 9 mm.

Fig. 3 Schematic of the fabrication of the reagent-loaded one-channel μPAD for point-of-care aptamer-based adenosine assay with the glucometer readout.

Fig. 4 (A) Comparison of the relative glucose-producing efficiencies of α-, β-, and γ-amylase applied to hydrolyze amylose solutions at the same concentrations. (B) Glucometer signals

obtained from the zones c and d of several μPADs used for a control sample (PBS buffer without the analyte) and an adenosine sample (400 μM), severally.

Fig. 5 (A) The linear relationship between the glucometer signals obtained from the detection of different samples with the developed point-of-care assay and the concentrations of adenosine ($C_{adenosine}$). A linear calibration curve from 0 to 900 μM (with a regression equation of $y = 0.0349x + 0.8381$, R = 0.9965) was obtained. (B) Glucometer responses of the new assay to the control (PBS buffer without adenosine), 2 mM cytidine and uridine, and 240 μM adenosine. The error bars reflect the standard deviations from three repetitive experiments of each sample.

Videos S1 The first type of adjustment of the 4-channel fabrication face.

Videos S2 The second type of adjustment of the 4-channel fabrication face.

Videos S3 The third type of adjustment of the 4-channel fabrication face.

Videos S4 The fourth type of adjustment of the 4-channel fabrication face.

Videos S5 The first type of adjustment of the 8-channel fabrication face.

Videos S6 The second type of adjustment of the 8-channel fabrication face.

Videos S7 The third type of adjustment of the 8-channel fabrication face.

Videos S8 The fourth type of adjustment of the 8-channel fabrication face.

Videos S9 The first type of adjustment of the 16-channel fabrication face.

Videos S10 The second type of adjustment of the 16-channel fabrication face.

Videos S11 The third type of adjustment of the 16-channel fabrication face.

Videos S12 The fourth type of adjustment of the 16-channel fabrication face.

Videos S13 The liquid flowing in the device created from the first type of adjustment of the 4-channel face.

Videos S14 The liquid flowing in the device created from the second type of adjustment of the 4-channel face.

Videos S15 The liquid flowing in the device created from the third type of adjustment of the 4-channel face.

Videos S16 The liquid flowing in the device created from the fourth type of adjustment of the 4-channel face.

Videos S17 The liquid flowing in the device created from the first type of adjustment of the 8-channel face.

Videos S18 The liquid flowing in the device created from the second type of adjustment of the 8-channel face.

Videos S19 The liquid flowing in the device created from the third type of adjustment of the 8-channel face.

Videos S20 The liquid flowing in the device created from the fourth type of adjustment of the 8-channel face.

Videos S21 The liquid flowing in the device created from the first type of adjustment of the 16-channel face.

Videos S22 The liquid flowing in the device created from the second type of adjustment of the 16-channel face.

Videos S23 The liquid flowing in the device created from the third type of adjustment of the 16-channel face.

Videos S24 The liquid flowing in the device created from the fourth type of adjustment of the 16-channel face.

Highlights

- **An equipment-free method was proposed for fabricating paper analytical devices.**
- **This method was inspired by the worldwide ubiquitous Rubik's Cube toy.**
- **A point-of-care aptamer-based assay with glucometer readout was designed.**
- **It allowed for quantitative detection within several minutes.**

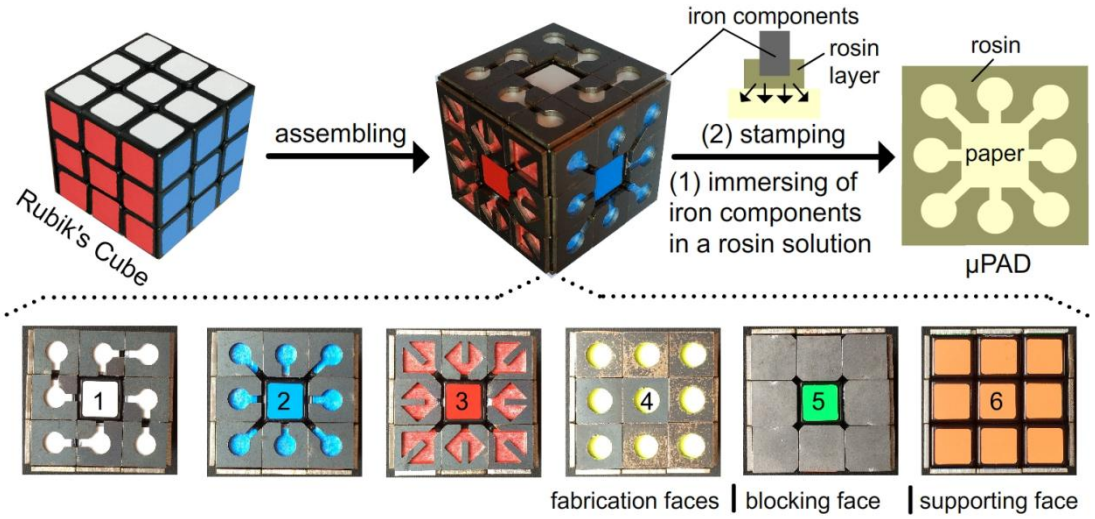
Rubik's Cube
assembling
iron components
rosin layer
(2) stamping
(1) immersing of iron components in a rosin solution
rosin
paper
μPAD
1
2
3
4
5
6
fabrication faces
blocking face
supporting face

Fig. 1

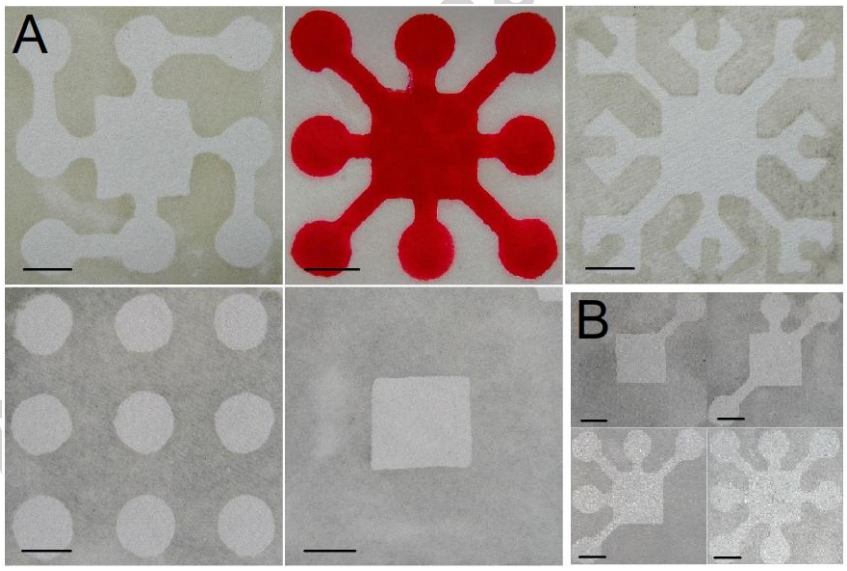
A
B

Fig. 2

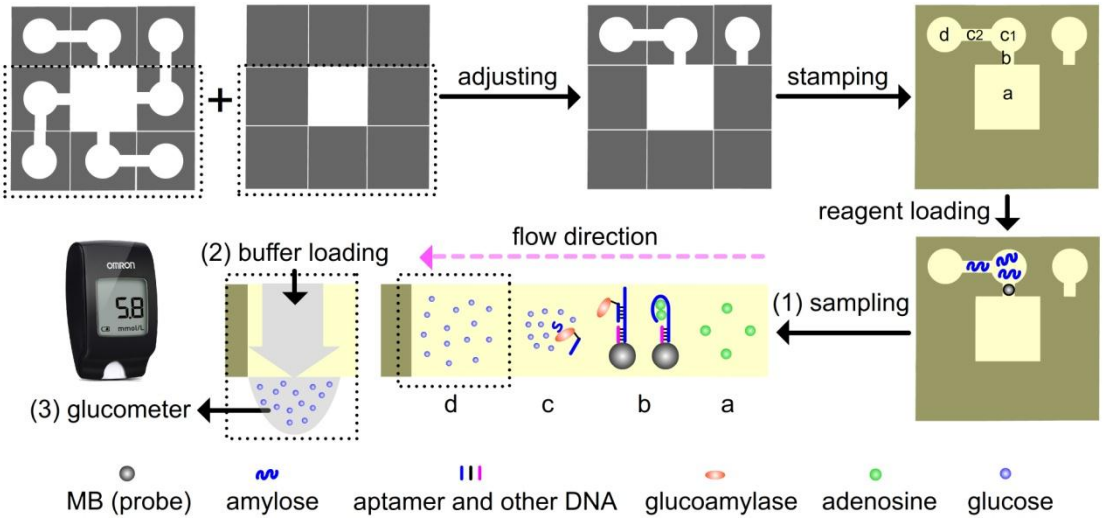

Fig. 3

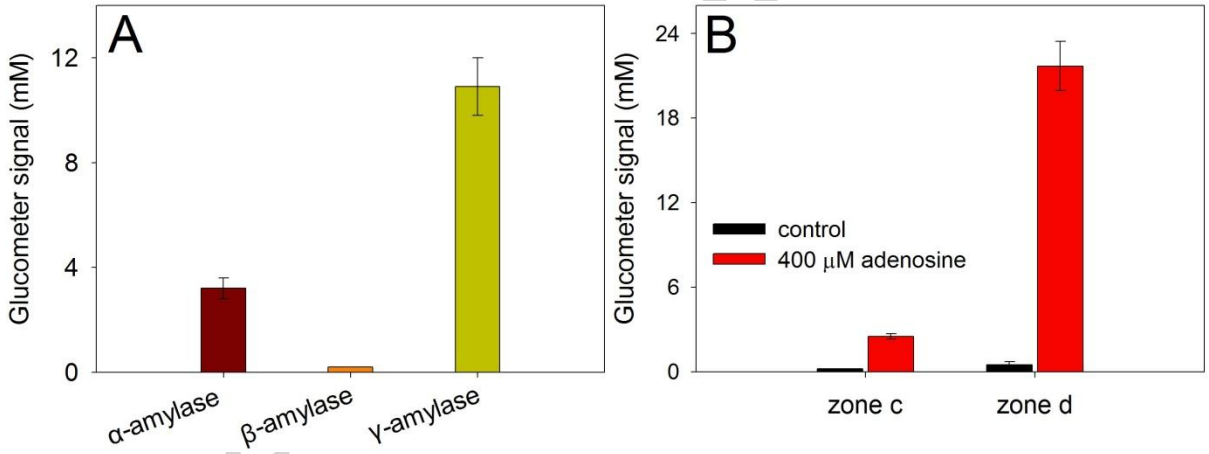

Fig. 4

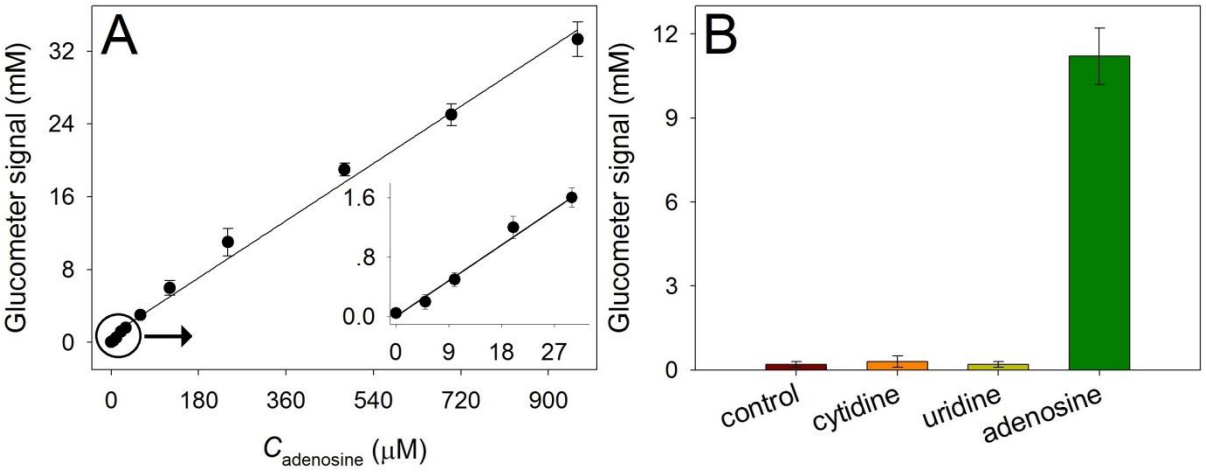

Fig. 5